GEOPHYSICAL RESEARCH LETTERS, VOL. 18, NO. 4, PAGES 701–704, APRIL 1991

VORTICITY AND DIVERGENCE IN THE HIGH-LATITUDE UPPER THERMOSPHERE

J. P. Thayer
SRI International, Menlo Park, California

T. L. Killeen
Department of Atmospheric, Oceanic, and Space Sciences, The University of Michigan

Abstract. Measurements made from the Dynamics Explorer-2 satellite in November 1981 through January 1982 and November 1982 through January 1983 have been analyzed to determine the divergence and vertical component of vorticity of the high-latitude neutral wind field in the upper thermosphere for quiet ($Kp \leq 3$) and active ($3+ \leq Kp \leq 6$) geomagnetic conditions and for both northern (winter) and southern (summer) hemispheres. This analysis provides the first experimental determination of the large-scale vorticity and divergence patterns in the polar thermosphere and provides insight into the relative strengths of the different sources of momentum and energy responsible for driving the winds. The principal findings from this work include the following: The mean neutral wind pattern is dominated by rotational flow rather than by divergent flow, with a typical vorticity : divergence ratio of ~2:1 for active conditions and ~4:1 for quiet conditions. Comparison of the divergence and vorticity patterns for quiet and active conditions indicates that the divergent component of the neutral flow intensifies more significantly with increasing geomagnetic activity than does the rotational component.

Introduction

Observations made during solar-cycle maximum from the low-altitude, polar-orbiting, Dynamics Explorer-2 (DE-2) spacecraft have shown that ionosphere-thermosphere coupling processes profoundly affect the high-latitude upper thermospheric neutral wind system. Because of ion drag, the thermospheric neutral winds at high latitudes tend to mimic the F-region high-latitude ion convection pattern and, thereby, develop similar vortex structures (see Killeen and Roble, 1988). The characteristics of the high-latitude neutral wind field during quiet and moderate geomagnetic activity have been reasonably well documented by satellite and ground-based observations (e.g., Killeen et al., 1982; Hays et al., 1984; Sica et al., 1986; Hernandez et al., 1990) and in modeling studies (e.g., Roble et al. 1982).

We have extended this previous work and here present the first large-scale experimental determinations of divergence and the vertical component of vorticity in the polar thermosphere for periods of both quiet and enhanced geomagnetic activity. Because the high-latitude ion-drag momentum forces are largely divergence-free (Rishbeth and Hanson, 1974) and the pressure-gradient forces induced by EUV absorption and Joule heating are largely curl-free in character, the derived vorticity and divergence fields provide separate insight into the relative strengths of the respective sources of momentum. We note that this correspondence between momentum source and the kinematic components of the flow should not be taken as perfect, however, since the Coriolis force acts to couple the divergent and rotational motion.

Several previous theoretical studies have been made of vorticity and divergence in the high-latitude thermosphere. Roble et al. (1982) calculated the vorticity and divergence fields from a simulated wind field forced only by ion drag and concluded that the generated neutral wind field at F-layer altitudes from a nondivergent momentum source was mostly nondivergent. Mayr and Harris (1978) used an analytic model to show that, while ion drifts induce horizontal winds that are predominantly divergence-free and give rise to small pressure variations, Joule heating is mainly responsible for the divergent wind field and strong pressure variations. Larsen and Mikkelsen (1987) used a two-dimensional, linear version of the shallow-water equations along with a vertical structure equation, excluding the effects of Joule heating, and determined that the nondivergent component of the high-latitude neutral wind is greater than the irrotational component by two orders of magnitude in the F-region.

In the following sections, we briefly describe the process used to derive the experimental high-latitude vorticity and divergence fields and discuss the significance of the derived fields.

Neutral Wind Observations

The meridional and zonal components of the thermospheric neutral wind were measured on satellite DE-2 using a Fabry-Perot interferometer or FPI and a wind and temperature spectrometer or WATS (Spencer et al., 1981), respectively. All resulting DE-2 neutral wind vector measurements between 300 and 550 km altitude for all Universal Times were binned and averaged in geomagnetic coordinates for two 3-month periods centered on December solstice in 1981-1982 and 1982-1983, assuming altitude independence above 300 km. The data were independently analyzed for quiet geomagnetic conditions ($Kp \leq 3$) and moderately active conditions ($3+ \leq Kp \leq 6$) and the bin size was 5° magnetic latitude (MLAT) and 1 hour magnetic local time (MLT). The use of geomagnetic coordinates for the neutral wind measurements was prompted by the previous results of Killeen et al. (1982) and Hays et al. (1984) who showed that the neutral wind field at high latitudes could best be described in such coordinates.

The data correspond to B_z "southward" conditions where only data in which the IMF $B_z \leq +1$ nT were considered, irrespective of the sign of the B_y component, thus avoiding the distorted or multicellular ion convection geometries associated with B_z northward. For a specific orbit to be included, both the corresponding Kp and B_z values were required to fall within their designated limits for a 2-hour period prior to each orbital pass. In this way, orbital passes were excluded if significant changes in neutral circulation due to rapidly changing IMF or

Paper number 91GL00131
0094-8534/91/91GL-00131$03.00

geomagnetic activity levels occurred. The total number of orbital passes used was 620 for the low *Kp* case, with most of the data in the 1+ to 3- range, and 388 for the high *Kp* case, with most of the data in the 4- to 6+ range.

An example of one of the averaged neutral wind fields is shown in Figure 1a for southern hemisphere, high *Kp* conditions. The wind field is displayed in a geomagnetic coordinate system with the co-rotation vector removed and is viewed from above the north pole through a transparent earth, so that, the wind vortices are of the same sense for both hemispheres. Figure 1a illustrates clearly the large-scale vortex associated with the dusk cell of ionospheric convection, previously reported by many authors [e.g. see Killeen and Roble (1988) and references therein].

The nature of the DE-2 orbit is such that little or no experimental data were available for some areas of the geomagnetic polar dial. For example, in Figure 1a, the regions below about 50° geomagnetic latitude in the noon and midnight sectors were undersampled. To obtain full vorticity and divergence maps for the northern and southern high-latitude regions above 40° (geomagnetic), we developed a technique to incorporate model wind values derived from the Vector Spherical Harmonic (VSH) model of Killeen et al. (1987) in areas where there were no measurements. In this manner, the experimental wind fields were augmented with VSH model values (primarily at middle and low latitudes) and global gridded wind fields were thereby obtained for the two cases of low and high geomagnetic activity. The merged experiment-model global wind fields were then smoothed by first fitting the fields to a set of vector spherical harmonic basis functions and then regenerating the individual fields using a limited set of coefficients (truncated at degree n=25 and order m=5). The experiment-model merger and spectral truncation scheme are fully described by Thayer and Killeen (1991).

Figure 1b shows the results of the application of the data-handling technique to the wind field of Figure 1a. A comparison of Figures 1a and 1b illustrates the smooth nature of the final high-latitude wind field and the fidelity with which the measured wind field (Fig. 1a) is reproduced by the spectrally analyzed and regenerated field (Fig. 1b). Four such wind fields were obtained in this way for northern and southern hemispheres and for quiet and active geomagnetic conditions.

Vorticity and Divergence Analysis

Vorticity is a measure of the microscopic rotation in the flow generated by shear, with positive values representing cyclonic rotation and negative values representing anticyclonic rotation. Divergence is related to the acceleration or deceleration of the winds. A positive divergence represents acceleration of the local winds and a negative divergence (convergence) represents deceleration of the local winds. Thus, the vorticity and divergence provide basic underlying flow configurations to help elucidate the momentum sources that ultimately determine the total wind field.

In spherical coordinates the divergence, D, and the vertical component of the vorticity, ζ, are given respectively as,

$$D = \nabla \cdot \vec{V} = \frac{1}{\sin\theta}\left\{\frac{\partial}{\partial\theta}(v_\theta \sin\theta) + \frac{\partial v_\phi}{\partial\phi}\right\} \quad (1)$$

$$\xi = (\vec{r} \times \nabla) \cdot \vec{V} = \frac{1}{\sin\theta}\left\{\frac{\partial}{\partial\theta}(v_\phi \sin\theta) + \frac{\partial v_\theta}{\partial\phi}\right\}$$

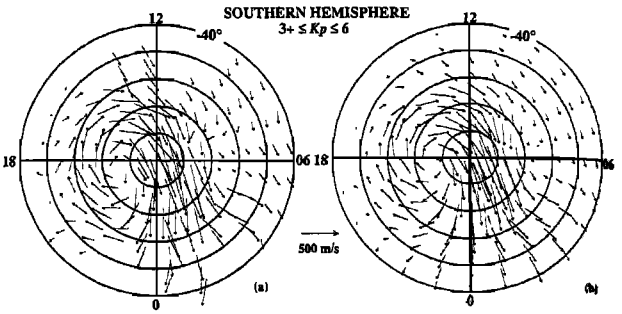

Fig. 1. (a) Empirical neutral wind pattern in geomagnetic polar coordinates for the southern hemisphere. (b) The same data after the manipulation and smoothing procedure described in the text.

where $\vec{r}$ is the unit vector in the vertical direction, ∇ is the two-dimensional horizontal Del operator, θ is the colatitude, ϕ is the longitude, v_θ is the meridional wind, and v_ϕ is the zonal wind. The derivation of vorticity and divergence from the averaged DE-2 wind field, such as that shown in Figure 1b, is readily evaluated using the derivative properties of the vector spherical harmonic coefficients (cf. Swarztrauber, 1981).

The derived divergence and vertical component of vorticity patterns for quiet and active conditions in the northern (winter) hemisphere are shown in Figure 2 and those for the southern

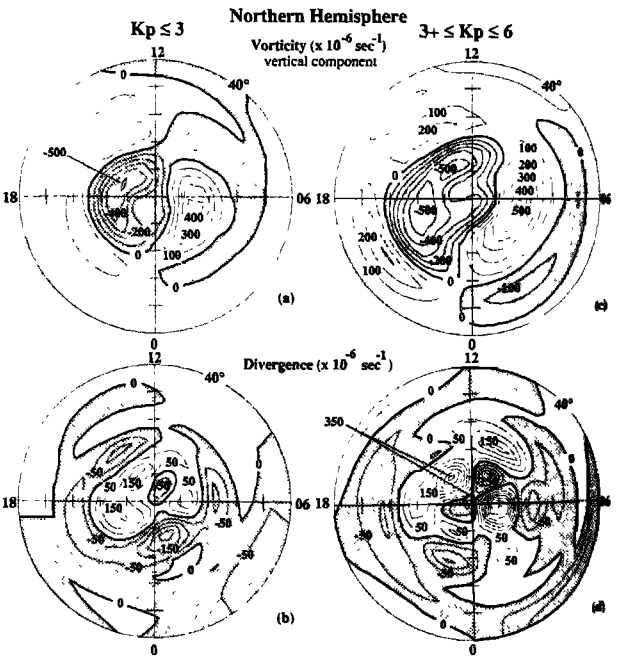

Fig. 2. Northern (winter) hemisphere plot in geomagnetic coordinates of (a) derived vertical component of vorticity for geomagnetically quiet conditions (contour interval of 100×10^{-6} sec $^{-1}$); (b) corresponding derived divergence (contour interval of 50×10^{-6} sec^{-1}); (c) derived vertical component of vorticity for geomagnetically active conditions; (d) corresponding derived divergence. The zero contour is given by the bold line. Anticyclonic flow and convergent flow are identified by the hatched region.

(summer) hemisphere in Figure 3. The derived vorticity pattern shown in Figure 2a, with a contour interval of 100×10^{-6} sec^{-1}, describes the rotation in the northern hemisphere high-latitude neutral thermospheric wind field during low *Kp*, where negative (positive) vorticity denotes anticyclonic (cyclonic) rotation. Since vorticity is generated by wind shear, the strong antisunward flow over the magnetic pole bordered by sunward flow in the dawn and dusk sectors creates two regions of counterrotating flow. Negative vorticity or anticyclonic rotation occurs primarily in the dusk sector with a minimum value of -518×10^{-6} sec^{-1}, while positive vorticity or cyclonic rotation occurs in the dawn sector with a maximum value of 426×10^{-6} sec^{-1}. The dusk sector winds have a strong sunward component which enhances the shear and creates the largest values of vorticity in the neutral circulation. In the dawn sector, the vorticity is significant as a result of the strong latitudinal gradient in the zonal winds. The magnitudes of the maximum vorticity in the dawn and dusk sectors are surprisingly similar; however, the processes of vorticity generation in the two sectors are somewhat different. In the dawn sector, most of the vorticity is generated by shear as the wind speed normal to the flow changes, while in the dusk sector, the vorticity is generated mostly by curvature as the winds turn.

The contour of zero vorticity marks the region of shear reversals as the winds either reach a maximum in the antisunward direction near the inner polar region or a maximum in the sunward direction in the dawn and dusk sectors. Thus, the transition regions of vorticity are good indicators of the shear boundaries in the wind field and may be used to define the spatial dimensions of the high-latitude neutral circulation. Equatorward of 60° MLAT, the magnitude of vorticity is significantly reduced, illustrating the strong influence of the high-latitude ion convection in creating rotational motion in the neutral flow.

The derived divergence pattern is shown in Figure 2b with a similar format. Localized islands of divergence occur primarily in the high-latitude region above 65° MLAT, with positive divergence occurring near 14:00 MLT and in the 18-6 MLT plane. Negative islands of divergence or convergence exist near the noon-midnight meridian. The maximum divergence occurs in the dusk sector, with a value of 172×10^{-6} sec^{-1}, while the minimum divergence (or maximum convergence) occurs in the midnight sector with a value of -232×10^{-6} sec^{-1}. As with the vorticity pattern, the regions of divergence occur primarily at high latitudes, demonstrating the significance of the high-latitude heat sources in creating the divergence in the wind field. The divergence field is much more complex and significantly smaller in magnitude than the corresponding vorticity field.

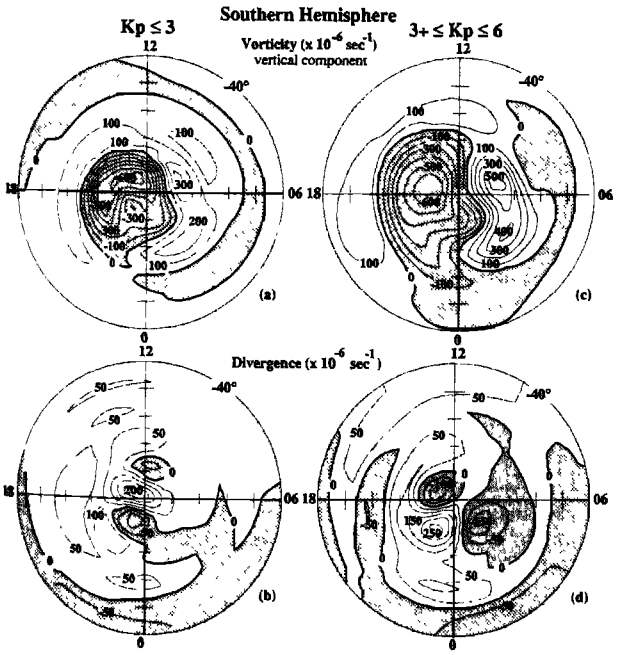

Fig. 3. Same display as Figure 2 for the southern (summer) hemisphere data set.

The vorticity (vertical component) field for high levels of geomagnetic activity in the northern hemisphere is illustrated in Figure 2c. For enhanced geomagnetic activity, the vorticity maximum in the dawn sector increases by 31% to 559×10^{-6} sec^{-1} while the vorticity minimum in the dusk sector decreases by 15% to -596×10^{-6} sec^{-1}. The vorticity enhancement is essentially due to increased antisunward wind speeds within the geomagnetic polar cap and increased sunward winds in the dawn and dusk sectors, associated with high geomagnetic activity. The spatial extent of the vorticity pattern for high *Kp* is greater than that for low *Kp*, extending below 60° MLAT, illustrating the expansion of the high-latitude wind field during elevated geomagnetic activity. This, in turn, is indicative of increased ion drag caused by enhanced and expanded electric fields known to occur during high geomagnetic activity (cf. Heppner and Maynard, 1987).

The divergence field determined from the neutral circulation during high geomagnetic activity in the northern hemisphere is illustrated in Figure 2d. This field illustrates enhancements of divergence in the 14 MLT region by 118% to 372×10^{-6} sec^{-1} and in the 6 MLT region by 212% to 403×10^{-6} sec^{-1} as well as enhancements of convergence in the prenoon sector by 176% to -207×10^{-6} sec^{-1} over the corresponding values for low *Kp*. These regions of enhanced divergence coincide with areas of typically strong Joule heating (e.g., Baron and Wand, 1983) and the divergence values are comparable in magnitude to the vorticity values found in those regions. The sharp percentage increases illustrate that the divergence field increases and intensifies more with geomagnetic activity than does the corresponding vorticity, indicating a stronger geomagnetic activity response for the energy input than the momentum input. This stronger response in the neutral divergence is indicative of the nonlinear nature of the Joule heating associated with the ion/neutral interactions. Other nongeomagnetic effects such as EUV heating and the Coriolis force, however, also strongly influence the relationship between vorticity and divergence in the wind field. The convergence region in the prenoon sector indicates a reduction in the wind speeds as the flow enters the geomagnetic polar cap. This reduction may be caused by possible ion-drag processes or by forced convergence from the two localized regions of divergence on either side of this region.

Overall, the vorticity : divergence ratio for the low K_p case (Figs. 2a and 2b) is about 4:1 while for the high K_p case (Figs. 2c and 2d), the ratio is only about 2:1 and even less in localized regions. It may be inferred from these results that the high-latitude thermosphere during active times is strongly influenced by the momentum sources of ion convection, day to night pressure gradient, as well as localized pressure gradient forces

set-up by high-latitude heating. A comparison of these vorticity and divergence fields with the localized measurements of Larsen et al. (1989), taken approximately at 74° MLAT 5 MLT, illustrates similar magnitude and sign in the vorticity, indicative of cyclonic flow and dawn sector circulation, but shows disagreement in the divergence.

Figure 3 shows the divergence and vertical component of vorticity maps for the southern (summer) hemisphere region in the same format as for the northern hemisphere results. Many of the comments made for the northern hemisphere results pertain also to the southern hemisphere. A comparison between the results for the two hemispheres indicates that the derived vorticity patterns are similar and that, while both hemispheres show localized regions of strong positive and negative divergence, there are significant hemispheric differences in morphology for the divergence fields.

Conclusions

Measurements made from the DE-2 satellite in November 1981 through January 1982 and November 1982 through January 1983 have been analyzed to determine the divergence and the vertical component of vorticity of the high-latitude neutral wind field in the upper thermosphere for quiet ($Kp \leq 3$) and active ($3+ \leq Kp \leq 6$) geomagnetic conditions and for both northern (winter) and southern (summer) hemispheres. This analysis of the derived vorticity and divergence patterns for the high-latitude neutral thermospheric circulation has led to the following conclusions:

(1) The dynamics of the high-latitude neutral thermosphere are dominated by rotational motion, imparted primarily through the ion drag force, rather than by divergent motion, imparted primarily through the pressure gradient force set-up by Joule and solar heating.

(2) For quiet geomagnetic conditions, the typical vorticity : divergence ratio is on the order of 4:1.

(3) For active geomagnetic conditions, the typical vorticity : divergence ratio is on the order of 2:1 over much of the polar region, but significantly smaller in localized regions of the dawn and postnoon sectors, where the divergent motion induced by local heat sources becomes comparable in magnitude to the rotational motion.

(4) Divergence in the high-latitude thermosphere increases and intensifies more with increasing geomagnetic activity than does vorticity, indicating a larger response of the thermospheric wind system to enhancements in the energy input associated with elevated geomagnetic activity than for the corresponding momentum input.

Acknowledgments. This work was supported by NASA Grant NAG5-465 and by NSF Grant ATM-8918476 to the University of Michigan. The WATS data were kindly provided by N. W. Spencer and L. E. Wharton.

References

Baron, M.J. and R.H. Wand, F region ion temperature enhancements resulting from Joule heating, *J. Geophys. Res., 88,* 4114-4118, 1983.

Hays, P.B., T.L. Killeen, N.W. Spencer, L.E. Wharton, R.G. Roble, B.E. Emery, T.J. Fuller-Rowell, D. Rees, L.A. Frank, and J.D. Craven, Observations of the dynamics of the polar thermosphere, *J. Geophys. Res., 89,* 5597-5612, 1984.

Heppner, J.P., and N.C. Maynard, Empirical high latitude electric field models, *J. Geophys. Res., 92,* 4467-4489, 1987.

Hernandez, G., R.W. Smith, R.G. Roble, J. Gress, and K.C. Clark, Thermospheric Dynamics at the South Pole, *Geophys. Res. Lett., 17,* 1255-1258, 1990.

Killeen, T.L. and R.G. Roble, Thermosphere dynamics driven by magnetospheric sources: contributions from the first five years of the Dynamics Explorer program, *Rev. Geophys. Space Phys., 26,* 329-367, 1988.

Killeen, T.L., P.B. Hays, N.W. Spencer, and L.E. Wharton, Neutral winds in the polar thermosphere as measured from Dynamics Explorer, *Geophys. Res. Lett., 9, 957-960,* 1982.

Killeen, T.L., R.G. Roble, and N.W. Spencer, A Computer model of global thermospheric winds and temperatures, *Adv. Space Res., 7,* 207-215, 1987.

Larsen, M.F. and I.S. Mikkelsen, The normal modes of the thermosphere, *J. Geophys. Res., 92,* 6023-6043, 1987.

Larsen, M.F., I.S. Mikkelsen, J.W. Meriwether, R. Niciejewski, and K. Vickrey, Simultaneous observations of neutral winds and electric fields at spaced locations in the dawn auroral oval, *J. Geophys. Res., 94,* 17235-17243, 1989.

Mayr, H.G. and I. Harris, Some characteristics of electric field momentum coupling with the neutral atmosphere, *J. Geophys. Res., 83,* 3327-3336, 1978.

Rishbeth, H., and W.B. Hanson, A comment on plasma 'pile-up' in the F-region, *J. Atmos. Terr. Phys., 36,* 703-706, 1974.

Roble, R.G., R.E. Dickinson, and E.C. Ridley, Global circulation and temperature structure of thermosphere with high-latitude plasma convection, *J. Geophys. Res., 87,* 1599-1614, 1982.

Sica, R.J., M.H. Rees, G.J. Romick, G. Hernandez, and R.G. Roble, Auroral zone thermospheric dynamics: 1. Averages, *J. Geophys. Res., 91,* 3231-3244, 1986.

Spencer, N. W., L. E. Wharton, H. B. Niemann, A. E. Hedin, G. R. Carignan, and J. C. Maurer. The Dynamics Explorer wind and temperature spectrometer, *Space Sci. Instrum., 5,* 417-428, 1981.

Swarztrauber, P.N., The approximation of vector functions and their derivatives on the sphere, *SIAM J. Numer. Anal., 18,* 191-210, 1981.

Thayer, J.P., and T.L. Killeen, A Kinematic Analysis of the High-Latitude Neutral Thermospheric Circulation, submitted to *J. Geophys. Res.*, 1991.

T. L. Killeen, Space Physics Research Laboratory, Department of Atmospheric, Oceanic and Space Sciences, The University of Michigan, 2455 Hayward, Ann Arbor, MI 48109.

J. P. Thayer, Geoscience and Engineering Center, SRI International, 333 Ravenswood Avenue, Menlo Park, California 94025.

(Received November 21, 1990;
accepted January 4, 1991.)